

# Design of Low $V_\pi$ High-Speed GaAs Travelling-Wave Electrooptic Phase Modulators Using an n-i-p-n Structure

Qiaoyin Lu, Weihua Guo, Diarmuid Byrne, and John F. Donegan, *Senior Member, IEEE*

**Abstract**—GaAs-based electrooptic phase modulators using an n-i-p-n structure and coplanar waveguide traveling-wave electrodes are designed using the compact 2-D finite-difference time-domain technique and Padé approximation transform. By optimization, an electrical 3-dB bandwidth of 40 GHz and a 6.6-V  $V_\pi$  are predicted for a 5-mm-long modulator.

**Index Terms**—Electrooptic modulator, Padé approximation transform, 2-D finite-difference time-domain (FDTD) method, traveling-wave (TW) electrodes.

## I. INTRODUCTION

HIGH-SPEED semiconductor optical modulators are very important components for optical communication systems [1]. Characteristics such as low drive voltage, wide bandwidth, low insertion loss, low wavelength and temperature sensitivity, and low cost are essential for these optical modulators. InP-based modulators are very attractive because they are generally more compact and have lower half-wavelength voltage ( $V_\pi$ ) compared with GaAs and LiNbO<sub>3</sub>-based modulators. Ten-gigahertz InP Mach-Zehnder (MZ) intensity modulators using additional imbalance control electrodes and working with zero chirp across the whole C-band have been reported [2]. Forty-gigahertz InP modulators have also been reported which use an n-i-n waveguide structure instead of the conventional p-i-n structure to reduce both the microwave and optical losses. By utilizing the large electrooptical coefficients due to the quantum-confined Stark effect, 40-GHz operation with a drive voltage of only 2.3 V has been achieved [3]. These InP-based modulators have the drawback of the wavelength dependence of the drive voltage and generally need additional electric control to eliminate this wavelength dependence. GaAs-based modulators do not have this problem due to its larger bandgap energy. For GaAs modulators, the general structure used is the Schottky-i-n (Schottky) structure [1], [4], [5], with capacitively loaded coplanar strip line electrodes [1] or coplanar waveguide (CPW) electrodes [5]. Since a complex configuration is introduced into the electrodes high accuracy is required in fabrication. To date such a modulator

has been demonstrated with a 35-GHz optical bandwidth and  $5 \text{ V} \cdot \text{cm}^{-1} V_\pi$  [5]. In this letter, we report a new design for GaAs modulators based on an n-i-p-n structure. The travelling-wave (TW) CPW electrodes are employed to realize the high speed operation. The structure is simple to fabricate and should provide cost advantages. The compact 2-D finite-difference time-domain (FDTD) method and Padé approximation transform is used for the design. By optimization, an electrical 3-dB bandwidth of nearly 40 GHz (optical 3-dB bandwidth of 80 GHz) and a  $V_\pi$  around 6.6 V are predicted for a 5-mm-long phase modulator.

## II. 2-D FDTD AND PADÉ TRANSFORM

The compact 2-D FDTD technique [6] can efficiently analyze arbitrary guided-wave structures which are uniform in the propagation direction. In compact 2-D FDTD, the field dependence on the propagation direction is represented by a phase factor  $\exp(-j\beta z)$ , where  $\beta$  is the propagation constant, so that all 3-D electromagnetic fields can be represented by a 2-D mesh, which can greatly reduce the computer memory use and computation time. By using a variable transform, the solver can run with real variables; therefore, the memory requirement and computation time can be further reduced. For a general lossy waveguide structure, the discrete equations for the electromagnetic fields in 2-D meshes are expressed as (for simplicity, just  $E_x$  is listed which is the main electric field component of the quasi-transverse-electromagnetic (TEM) mode of a CPW structure)

$$\begin{aligned}
 E_{x,i+0.5,j}^{n+1} &= b_0 E_{x,i+0.5,j}^n \\
 &\quad + b_1 (H_{z,i+0.5,j+0.5}^{n+0.5} - H_{z,i+0.5,j-0.5}^{n+0.5}) \\
 &\quad + b_2 H_{y,i+0.5,j}^{n+0.5} \\
 b_0 &= \frac{2\varepsilon - \sigma\Delta t}{2\varepsilon + \sigma\Delta t} \\
 b_1 &= \frac{2\Delta t}{(2\varepsilon + \sigma\Delta t)\Delta y}, b_2 = \frac{2\beta\Delta t}{2\varepsilon + \sigma\Delta t} \quad (1)
 \end{aligned}$$

where the superscript  $n$  and subscripts  $i$  and  $j$  are indexes indicating the time step, space steps in the  $x$  and  $y$  direction, respectively;  $\Delta t$  and  $\Delta y$  are corresponding step lengths;  $\varepsilon = \varepsilon_0\varepsilon_r$ ;  $\mu_0$  and  $\varepsilon_0$  are the permeability and permittivity in vacuum;  $\varepsilon_r$  and  $\sigma$  are the relative dielectric constant and electric conductivity of the material. By iteration, the field evolution with time can be simulated with the obtained data transformed into the frequency domain to find the mode information of the modeled structure. FFT is the tool generally used for this transformation, however, it is inefficient for high frequency resolution. A transformation based on the Padé approximation was employed to overcome

Manuscript received May 08, 2008; revised July 10, 2008. First published September 3, 2008; current version published October 15, 2008. This work was supported by SFI under its CSET Centre for Telecommunication Value Driven Research (CTVR), Grant 03/IE3/I405.

The authors are with the Semiconductor Photonics Group, School of Physics and Centre for Telecommunication Value-Chain Driven Research (CTVR), Trinity College, Dublin 2, Ireland (e-mail: luqi@tcd.ie).

Color versions of one or more of the figures in this letter are available online at <http://ieeexplore.ieee.org>.

Digital Object Identifier 10.1109/LPT.2008.2005009

TABLE I  
WAFER STRUCTURE

Material	Thickness ( $\mu\text{m}$ )	Doping ( $\text{cm}^{-3}$ )	Refractive Index
GaAs	0.2	$1 \times 10^{18}$ (n)	3.377
$\text{Al}_{0.41}\text{Ga}_{0.59}\text{As}$	1.0	$1 \times 10^{18}$ (n)	3.171
$\text{Al}_{0.41}\text{Ga}_{0.59}\text{As}$	0.45	Depleted	3.171
GaAs	0.4	Depleted	3.377
$\text{Al}_{0.41}\text{Ga}_{0.59}\text{As}$	0.45	Depleted	3.171
$\text{Al}_{0.6}\text{Ga}_{0.4}\text{As}$	0.2	$1 \times 10^{18}$ (p)	3.079
$\text{Al}_{0.41}\text{Ga}_{0.59}\text{As}$	2	$1 \times 10^{18}$ (n)	3.171
GaAs	0.5	$1 \times 10^{18}$ (n)	3.171
Sub GaAs	350	(SI)	3.377

this problem which can greatly improve the frequency resolution [7]. In this letter, we use the Padé approximation transform to calculate the mode spectrum from which a Lorentz fitting can generate the mode frequency and quality factor ( $Q = f_0/\Delta f$ ,  $f_0$  and  $\Delta f$  are the center frequency and 3-dB bandwidth of the mode spectrum). The amplitude loss, effective index, and phase velocity of the modeled waveguide can, therefore, be calculated as

$$\alpha = \frac{\beta}{2Q}, \quad n_{\text{eff}} = \frac{\beta}{k_0}, \quad v_p = \frac{c}{n_{\text{eff}}} \quad (2)$$

where  $k_0$  and  $c$  are the wave number and light velocity in vacuum. The characteristic impedance of the modeled waveguide can be calculated based on the power-current definition  $Z_0 = P_0/|I|^2$ .

### III. TW PHASE MODULATOR DESIGN

#### A. *n-i-p-n Wafer Structure*

The wafer is configured with an n-i-p-n structure as listed in Table I. For electrical loss reduction, n-doped GaAs is introduced to make the Ohmic contact for both the signal and ground electrode. A 0.2- $\mu\text{m}$ -thick p-doped ( $1 \times 10^{18} \text{ cm}^{-3}$ )  $\text{Al}_{0.6}\text{Ga}_{0.4}\text{As}$  layer is used as the blocking layer to prevent current flowing between the cap and the lower n-GaAs contact layers [8]. The intrinsic layer is designed to be 1.3  $\mu\text{m}$  thick in a trade-off between wide bandwidth and low drive voltage operation.

#### B. *Optical Waveguide*

The optical waveguide employed is a deeply etched ridge waveguide with strong lateral optical confinement as schematically shown in Fig. 1. The width of the ridge is set to be 2  $\mu\text{m}$  for ease of fabrication. A 0.4- $\mu\text{m}$ -thick GaAs layer is designed as the waveguide core sandwiched by two 0.45- $\mu\text{m}$ -thick  $\text{Al}_{0.41}\text{Ga}_{0.59}\text{As}$  upper and lower confinement layers to confine the optical field in the vertical direction. Although having a strong lateral optical confinement, the waveguide is still a single-mode waveguide. The lower cladding layer is designed to be 2  $\mu\text{m}$  thick in order to reduce the loss caused by leakage into the high-index GaAs substrate. The beam propagation method (BPM) is used to analyze the optical waveguide. In Fig. 2(a), the calculated electric field distribution of the fundamental quasi-transverse-electric (TE) mode is plotted, which shows a very strong mode confinement in the intrinsic layer.

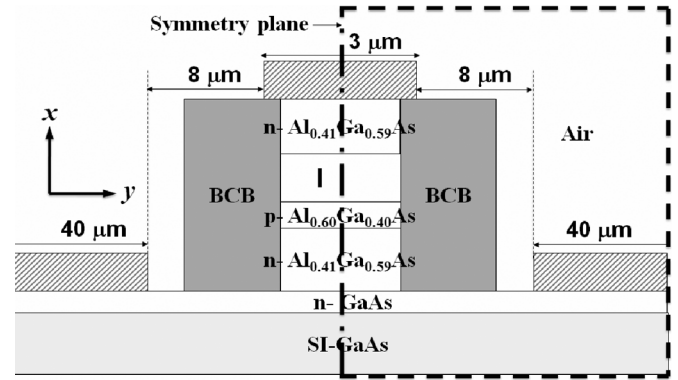


Fig. 1. Cross section of the designed CPW structure.

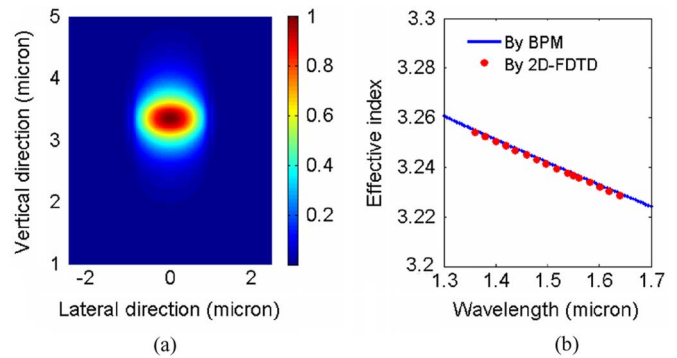


Fig. 2. (a) Contour plot of the electric field distribution of the quasi-TE mode. (b) Effective index of the quasi-TE mode versus wavelength calculated by the 2-D FDTD technique and the BPM method.

The fundamental quasi-TE mode has an effective index of 3.24, a group index and group velocity of about 3.5 and 8.57 cm/ns, respectively, at a wavelength of 1550 nm. The calculated optical confinement factor in the p-doped layer is around 0.5%. The additional loss caused by this p-doped layer is estimated to be around 0.6 dB/cm with an absorption coefficient of  $29 \text{ cm}^{-1}/10^{18} \text{ cm}^{-3}$  in p-doped GaAs at 1550 nm [9].

To verify our 2-D FDTD and Padé approximation transform program, the mode effective index dispersion of the fundamental quasi-TE mode was also analyzed by this 2-D FDTD method. To save computation time, just half of the waveguide structure was employed in the FDTD simulation. The symmetry plane vertically located at the center of the waveguide was set as an electric-field wall to simulate the quasi-TE mode. The results obtained are in very good agreement with the BPM method, as shown in Fig. 2(b).

#### C. *TW CPW Electrodes*

The CPW electrodes are chosen for the TW design due to their ease of fabrication. A cross section of the designed CPW structure is schematically shown in Fig. 1. The widths of the signal conductor are supported by bisbenzocyclobutene (BCB); the side ground conductor and the gap between the signal and ground are set to be 3, 40, and 8  $\mu\text{m}$  wide, respectively, which can ensure both impedance matching (50  $\Omega$ ) and velocity matching. The thickness of the Au signal and ground electrodes is 2  $\mu\text{m}$ . The relative permittivity of GaAs and BCB are taken as 12.9 and 2.6, respectively. The conductivities of the n-doped and p-doped layers are  $4.3 \times 10^4 \text{ S/m}$  and  $3.2 \times 10^3 \text{ S/m}$ . The

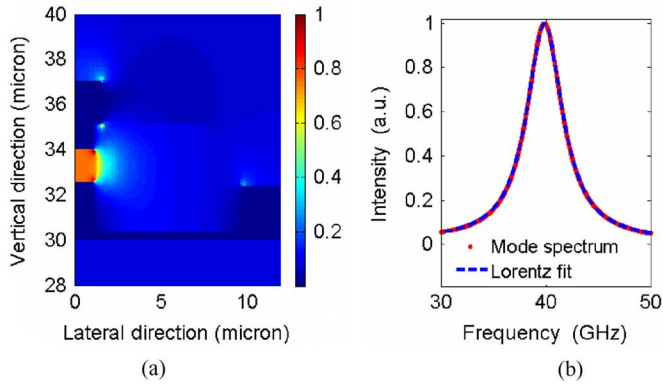


Fig. 3. (a) Contour plot of the electric field distribution of the quasi-TEM microwave mode. (b) Calculated mode spectrum and corresponding Lorentzian fitting.

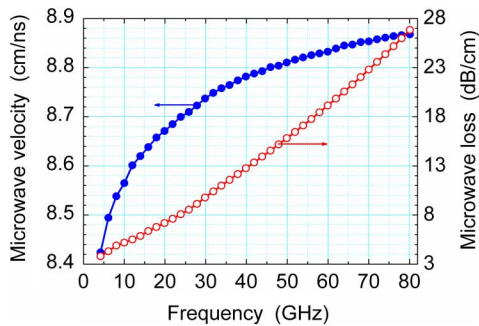


Fig. 4. Calculated microwave phase velocity and loss versus frequency.

compact 2-D FDTD method combined with the Padé approximation transform is used to simulate the CPW structure. To save computation time again, just half of the structure is simulated. A magnetic-field wall is employed at the vertical symmetry plane to simulate the quasi-TEM mode and Mur absorption boundary conditions are applied on all the other boundaries to absorb the outgoing waves as indicated in Fig. 1. Two-step meshes were employed. A fine mesh with a step of  $0.1 \mu\text{m}$  is used to describe the waveguide while a rough mesh with a step of  $0.5 \mu\text{m}$  is used to depict the GaAs substrate and the ground electrodes. Overall the mesh steps are less than  $1/2000$  of the microwave wavelength inside the material. The calculated microwave electric field distribution of the quasi-TEM mode in the CPW structure is presented in Fig. 3(a), which shows that the microwave electric field is mainly concentrated in the depletion region of the optical waveguide. The characteristic impedance calculated based on the power–current definition is close to  $50 \Omega$ . A typical mode spectrum calculated by the Padé approximation transform as well as the Lorentzian fitting is shown in Fig. 3(b).

Fig. 4 shows the calculated microwave loss and index versus frequency. The microwave loss increases with frequency, reaching  $5.2 \text{ dB/cm}$  at  $10 \text{ GHz}$  and  $12.7 \text{ dB/cm}$  at  $40 \text{ GHz}$ . The velocity mismatch to the optical wave is within  $4\%$  over the frequency range between  $5$  and  $80 \text{ GHz}$  for this design.

Fig. 5 shows the simulated frequency response of the designed modulator with a length of  $5 \text{ mm}$ . An electrical  $3\text{-dB}$  bandwidth of nearly  $40 \text{ GHz}$  and an optical  $3\text{-dB}$  bandwidth up to  $80 \text{ GHz}$  are predicted by the simulation. As the bandgap wavelength of GaAs is much shorter than the working wave-

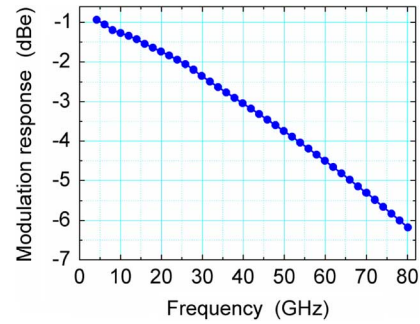


Fig. 5. Simulated frequency response of the designed  $5\text{-mm}$ -long phase modulator.

length ( $1550 \text{ nm}$ ), the linear electrooptic (LEO) effect is the main factor responsible for the induced index change. Since the intrinsic layer is just  $1.3 \mu\text{m}$  thick and nearly  $100\%$  overlapping between the optical mode and the microwave electric field, high modulation efficiency can be expected. For a  $5\text{-mm}$  modulation length, the calculated  $V_{\pi}$  is  $6.6 \text{ V}$  at the design wavelength assuming an LEO coefficient of  $1.42 \times 10^{-12} \text{ m/V}$  for GaAs. Across the whole  $C$ -band from  $1528$  to  $1568 \text{ nm}$ , the  $V_{\pi}$  variation is estimated to be only about  $0.25 \text{ V}$ .

#### IV. CONCLUSION

In summary, a  $5\text{-mm}$ -long GaAs TW electrooptic phase modulator with a  $3\text{-dB}$  electrical bandwidth of  $40 \text{ GHz}$  ( $3\text{-dB}$  optical bandwidth of  $80 \text{ GHz}$ ) and a  $V_{\pi}$  as low as  $6.6 \text{ V}$  is designed by the compact 2-D FDTD method and Padé approximation transform. The n-i-p-n structure used allows the modulator to have a thinner intrinsic layer ( $1.3 \mu\text{m}$ ) compared with the generally used Schottky-i-n structure which will produce a high modulation efficiency.

#### REFERENCES

- [1] R. G. Walker, "High-speed semiconductor intensity modulators," *IEEE J. Quantum Electron.*, vol. 27, no. 3, pp. 654–667, Mar. 1991.
- [2] I. Betty, M. G. Boudreau, R. Longone, R. A. Griffin, L. Langley, A. Maestri, A. Pujol, and B. Pugh, "Zero chirp  $10 \text{ Gb/s}$  MQW InP Mach-Zehnder transmitter with full-band tunability," in *Tech. Dig. OFC/NFOEC 2007*, pp. 179–181.
- [3] K. Tsuzuki, T. Ishibashi, T. Ito, S. Oku, Y. Shibata, T. Ito, R. Iga, Y. Kondo, and Y. Tohmori, "A  $40\text{-Gb/s}$  InGaAlAs-InAlAs MQW n-i-n Mach-Zehnder modulator with a drive voltage of  $2.3 \text{ V}$ ," *IEEE Photon. Technol. Lett.*, vol. 17, no. 1, pp. 46–48, Jan. 2005.
- [4] Y. Cui and P. Berini, "Modeling and design of GaAs traveling-wave electrooptic modulators based on the planar microstrip structure," *J. Lightw. Technol.*, vol. 24, no. 6, pp. 2368–2378, Jun. 2006.
- [5] J. Shin, S. Wu, and N. Dagli, "35-GHz bandwidth, 5-V-cm drive voltage, bulk GaAs substrate removed electrooptic modulators," *IEEE Photon. Technol. Lett.*, vol. 19, no. 18, pp. 1362–1364, Sep. 15, 2007.
- [6] S. Xiao and R. Vahldieck, "An efficient 2-D FDTD algorithm using real variables," *IEEE Microw. Guided Wave Lett.*, vol. 3, no. 5, pp. 127–129, May 1993.
- [7] W. Guo, W. Li, and Y. Huang, "Computation of resonant frequencies and quality factors of cavities by FDTD technique and Padé approximation," *IEEE Microw. Wireless Compon. Lett.*, vol. 11, no. 5, pp. 223–225, May 2001.
- [8] K. W. Goossen, J. E. Cunningham, and W. Y. Jan, "Single-layer structure supporting both heterojunction bipolar transistor and surface-normal modulator," *IEEE Photon. Technol. Lett.*, vol. 4, no. 4, pp. 393–395, Apr. 1992.
- [9] D. I. Babic, J. Piprek, K. Streubel, R. P. Mirin, N. M. Margalit, D. E. Mars, J. E. Bowers, and E. L. Hu, "Design and analysis of double-fused  $1.55\text{-}\mu\text{m}$  vertical-cavity lasers," *IEEE J. Quantum Electron.*, vol. 33, no. 8, pp. 1369–1383, Aug. 1997.